OPEN

Correspondence and
requests for materials
should be addressed to
G.S. (giancarlo.
salviati@cnr.it)

Porphyrin conjugated SiC/SiO$_x$ nanowires for X-ray-excited photodynamic therapy

F. Rossi[1], E. Bedogni[2], F. Bigi[2], T. Rimoldi[3], L. Cristofolini[3], S. Pinelli[4], R. Alinovi[4], M. Negri[1], S. C. Dhanabalan[1], G. Attolini[1], F. Fabbri[1], M. Goldoni[4], A. Mutti[4], G. Benecchi[5], C. Ghetti[5], S. Iannotta[1] & G. Salviati[1]

[1]IMEM-CNR Institute, Parco Area delle Scienze 37/A, 43124 Parma, Italy, [2]Chemistry Department, Parma University, Parco Area delle Scienze 17/A, 43124 Parma, Italy, [3]Physics and Earth Science Department, Parma University, Parco Area delle Scienze 7/A, 43124 Parma, Italy, [4]Department of Clinical and Experimental Medicine, Parma University, via Gramsci 14, 43126 Parma (Italy), [5]A.O.U. Parma Hospital, Department of Medical Physics, via Gramsci 14, 43126 Parma (Italy).

The development of innovative nanosystems opens new perspectives for multidisciplinary applications at the frontier between materials science and nanomedicine. Here we present a novel hybrid nanosystem based on cytocompatible inorganic SiC/SiO$_x$ core/shell nanowires conjugated *via* click-chemistry procedures with an organic photosensitizer, a tetracarboxyphenyl porphyrin derivative. We show that this nanosystem is an efficient source of singlet oxygen for cell oxidative stress when irradiated with 6 MV X-Rays at low doses (0.4–2 Gy). The in-vitro clonogenic survival assay on lung adenocarcinoma cells shows that 12 days after irradiation at a dose of 2 Gy, the cell population is reduced by about 75% with respect to control cells. These results demonstrate that our approach is very efficient to enhance radiation therapy effects for cancer treatments.

N anotechnology allows to create innovative systems with unique properties that can be applied in diverse sectors such as medicine, energy, electronics, environment, and consumer products (see e.g. ref. 1 and references therein enclosed). Concerning medical applications, during the last decade the ability to tailor the properties of materials allowed material scientists to propose new nanosystems with many potential benefits for human health in view of changing the way to diagnose, treat and image cancer cells[2–5].

Some proposals are nowadays under clinical trials since they stood in-vitro and in-vivo cyto-toxicity tests. Omitting the exciting genetic approach, radiation therapy and chemotherapy are still the most common and efficient cures to treat the uncontrolled growth and spread of cancer cells. The goal is to kill tumors while minimizing side effects. In this respect the recent development of new classes of multifunctional nanomaterials allowed the study of alternative approaches for cancer treatments.

Self Lighted Photodynamic Therapy (SLPDT) has been recently proposed in pilot studies[6–8] indicating that scintillation nanoparticles (NPs) can potentially be used to activate photodynamic therapy as a promising deep cancer treatment modality. SLPDT is a variation of the well assessed Photo Dynamic Therapy (PDT) usually used to "treat tumors on or just under the skin or on the lining of internal organs or cavities through the generation of an active form of oxygen (singlet oxygen) that destroys nearby cancer cells" (definition from the US-National Cancer Institute). In the SLPDT so far proposed in the literature, the light is generated by X-ray scintillation nanoparticles with attached photosensitizers. The photosensitizer (*e.g.* organic dyes and aromatic hydrocarbons, porphyrins, phthalocyanines and related tetrapyrroles etc., see *e.g.* ref. 9 and references therein enclosed) in the tumor absorbs the light and produces the singlet oxygen[10]. As X-rays can penetrate through tissue, deep tumors can be reached and treated. A possible drawback of the approach proposed[6–8] concern the use of scintillation particles that could not be totally biocompatible and that could not efficiently excite the absorption band of the attached photosensitizers to induce an efficient singlet oxygen generation.

Here we propose a hybrid nanosystem based on biocompatible[11] SiC/SiO$_x$ nanowires (NWs) functionalized via click chemistry procedures with tetra(N-propynyl-4-aminocarbonylphenyl)porphyrin (H$_2$TPACPP). Singlet oxygen generation activated by this nanosystem under 6 MV X-ray irradiation is experimentally verified in water solution. An effective Self Lighted Photo Dynamic Therapy is also demonstrated in a linear accelerator for
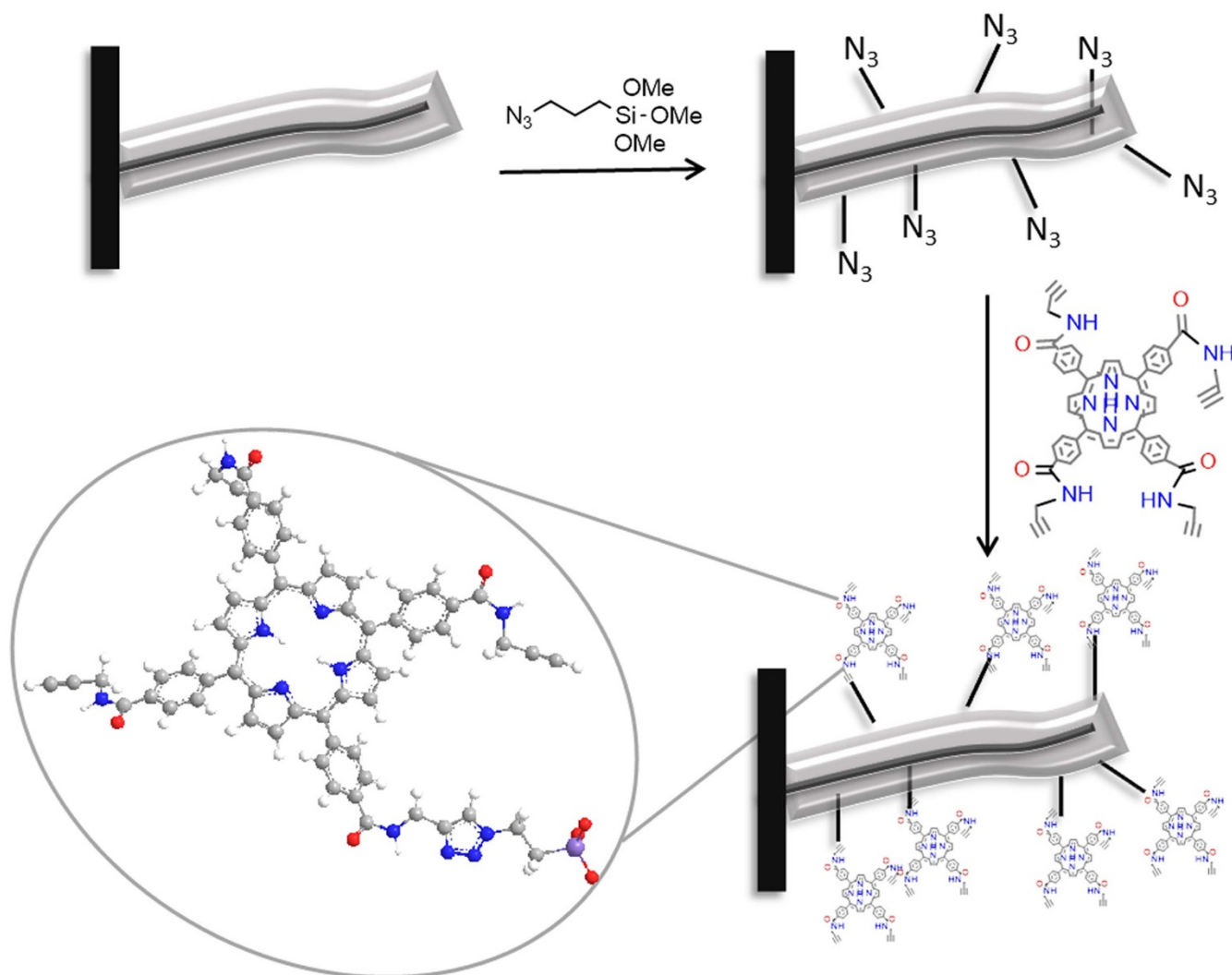
Figure 1 | Conjugation of porphyrin to SiC/SiOx NWs. Design of the SiC/SiOx/H$_2$TPACPP system: as-grown nanowires are functionalized with azide groups; the H$_2$TCPP porphyrin derivative containing C-C triple bonds (H$_2$TPACPP) is synthesized by converting the carboxy groups into N-propynylamides; the nanohybrid is constructed by bonding H$_2$TPACPP to the NWs.

Radiation Therapy, by in-vitro tests on lung cancer cells cultured with the functionalized NWs. This work validates the potential of our nanosystem in view of nanomedicine applications, aimed at the definition of more effective and synergic treatments of tumors deep inside the body.

Results and Discussion

Core-shell SiC/SiO$_x$ (1.8 < x < 2) NWs were grown on Silicon substrates in a CVD setup, using a Vapor-Liquid-Solid process catalysed by Iron[11]. This nanosystem presents an optical emission spectrum[12] which matches well the absorption bands of many organic photosensitizers and can be easily functionalized with inorganic crystals as well as with organic molecules[13,14].

Among the different photosensitizers, the class of porphyrins has a well-established application in photodynamic therapy, with initial approvals by the U.S. Food and Drug Administration. In this work we designed to link porphyrins to the SiC/SiO$_x$ NWs by the formation of covalent bonds *via* 1,3-dipolar cycloaddition reaction. Therefore azide functional groups were introduced on the NWs surface and carbon-carbon triple bonds in the phenyl rings of the porphyrin.

On the basis of the experience of some of the authors on the functionalization of amorphous and mesoporous silica with various organic compounds[15,16], the NWs as grown on the Si substrates were first activated with aq. HCl and then reacted with 3-azidopropyltri-methoxysilane by refluxing in toluene. Azide groups were bound to the NWs by condensation of alkoxysilyl groups with the hydroxyl groups present on the surface of the SiO$_x$ shell.

The selected porphyrin was the tetra(4-carboxyphenyl)porphyrin (H$_2$TCPP), and the carboxy groups were converted into amides containing a short chain with a terminal alkyne functional group. Indeed, to allow an efficient energy transfer from the nanowires to the photosensitizers, they have to be linked together and the distance between the donor and the acceptor should be less than 10 nm[8].

The carboxy groups of the porphyrin were first activated using EDCI/HOBt (EDCI: 1-(3-dimethylaminopropyl)-3-ethylcarbodiimide, HOBt: hydroxybenzotriazole), typical reagents employed for aminoacid condensation. The hydroxybenzotriazole ester of H$_2$TCPP, formed as intermediate, was in situ coupled with 2-propynylamine in the presence of dimethylaminopyridine (DMAP) in DMF at room temperature, affording tetra(N-propynyl-4-aminocarbonylphenyl)-porphyrin (H$_2$TPACPP). The porphyrin derivative was fully characterized.

The procedure employed to conjugate the porphyrin to the NWs is depicted in Figure 1.

The attachment of the photosensitizer to SiC/SiO$_x$ nanowires was accomplished on the basis of reactive group-matching, that is *via* the Huisgen 1,3 dipolar cycloaddition reaction giving the stable triazole
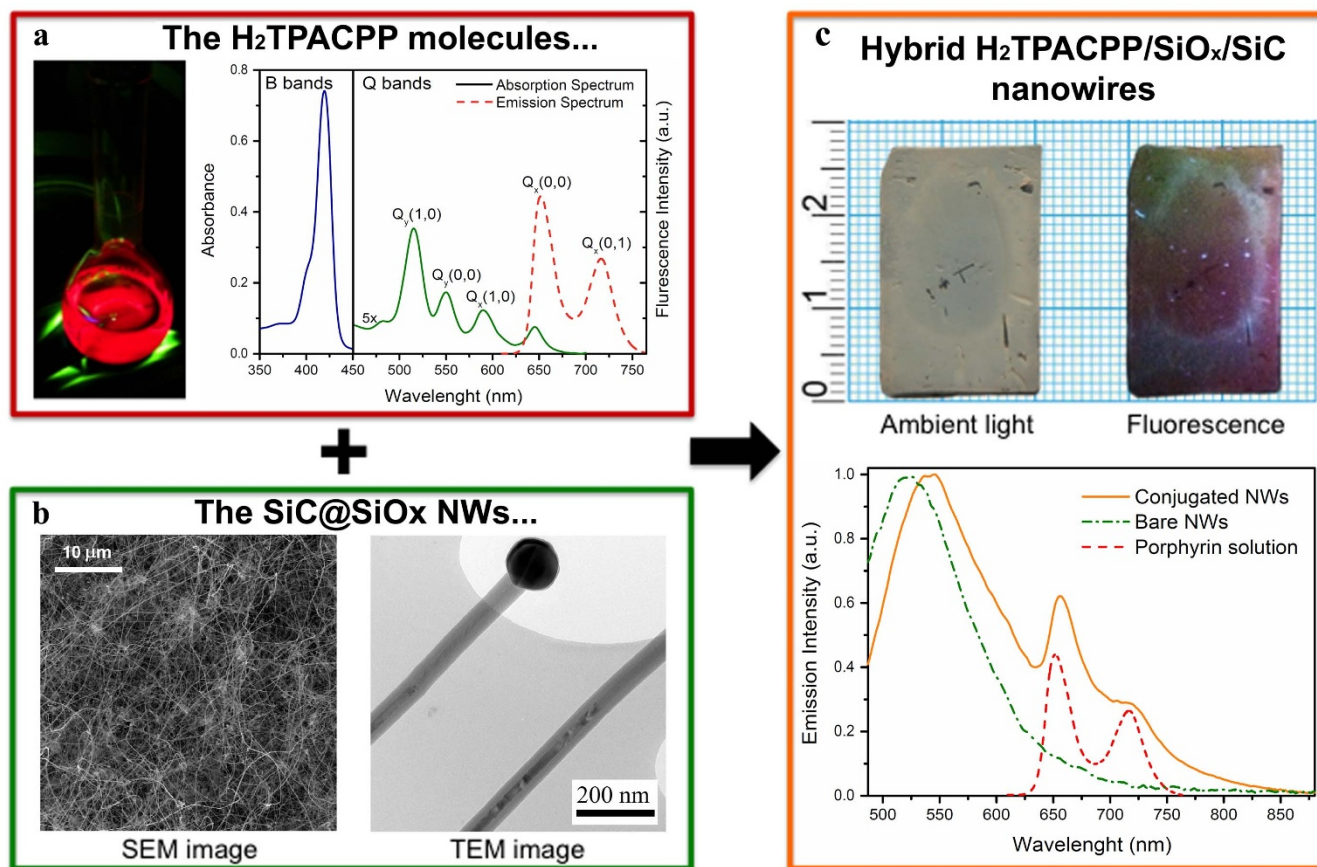
Figure 2 | Spectroscopic characterization of the NW-H2TPACPP system. (a) Picture: vial containing the H$_2$TPACPP porphyrin in dichloromethane solution, illuminated by a mercury-vapour lamp. Plot: Absorption (solid line) and Fluorescence (dashed line) spectra of the H$_2$TPACPP solution. (b) Left: SEM image of the as-grown NW network on Si substrate. Right: TEM image of two neighbour NWs over an holy-carbon support film. (c) Pictures: NW-H2TPACPP sample illuminated by ambient light (left) or mercury-vapour lamp (right). Plot: fluorescence spectra acquired at room temperature over as-grown NWs (dashed-dotted line) and NW-H$_2$TPACPP (solid line). The porphyrin emission (dashed line, from panel (a)) is also shown for sake of clarity.

(1,4- and 1,5-isomers) link. Thermal conditions, 160°C for 24 h, were preferred to Cu(I)-catalyzed click-reaction to avoid the metal insertion into the porphyrin core.

The characterization of the hybrid nanosystem and of its constituents is reported in Figure 2. The free porphyrin in dichloromethane solution has been studied by UV-VIS absorption and fluorescence emission spectroscopy (Figure 2a). The absorption spectrum contains the Soret-band at 420 nm ($S_0 \rightarrow S_2$, highly dipole allowed transition, blue line) and the Q-bands at 516, 550, 590 and 645 nm ($S_0 \rightarrow S_1$, weakly dipole allowed transition, green line amplified by a factor of 5). The superimposed emission spectrum (dashed line) from solution presents a small Stokes shift, estimated as:

$$\Delta E_{Stokes} = E^{Q(0,0)}{}_{abs} - E^{Q(0,0)}{}_{em} = 150 \pm 40 \text{ cm}^{-1} \qquad (1)$$

We identify the $Q_x(0,0)$ and $Q_x(0,1)$ emission peaks at 652 nm and 717 nm, respectively. These findings are consistent with the prediction of the classical four orbital model of free-base porphyrins[17,18] determined by the 2-fold symmetry of this substituted molecule.

Further, we have also verified that the linker does not influence the spectroscopic properties of the porphyrin, as reported in S.I. Figure S1.

The morphology of the inorganic component of the hybrid system has been assessed by SEM imaging (Figure 2b-left) showing that the NWs are arranged in dense tangles. TEM studies (Figure 2b-right) show that the NW structure is made by a crystalline 3C-SiC core (average diameter 20 nm) coated by an amorphous SiO$_x$ shell (average thickness 20 nm) with the catalyst nanoparticle tip.

Figure 2c-top shows the pictures of the hybrid nanosystem on large area (2.5 × 1.5 cm^2) silicon substrates, in ambient light (left) and in fluorescence conditions (excitation at 360 nm, right). In Figure 2c-bottom the comparison between the optical emissions from bare and conjugated NWs is reported.

The emission from bare NWs consists of a single large and unstructured peak centred at 523.5 nm, in excellent agreement with the near band-edge emission (NBE) of 3C-SiC[12]. The spectrum of the conjugated NWs clearly contains both contributions originating from the inorganic and organic components. The SiC NBE transition in the NW-H$_2$TPACPP nanosystem is red-shifted to 545 nm. A similar red-shift has been reported by other authors[19] and in the present case can be partly due to screening effects of the covering porphyrin due to Q-bands absorption.

Comparing the porphyrin contributions to the emission spectrum of the nanosystem with the fluorescence of the same molecule in solution, one can note a small red shift, in agreement with 8, and a slight broadening of the peaks. This suggests important steric effects due to the bonding, as discussed in greater detail in S.I.

As optical excitation is performed at 473 nm, i.e. inside the absorption of NWs but out of the main absorption band of porphyrin, the observed fluorescence, which has indeed a contribution from porphyrin, has to be ascribed to some form of electronic coupling between the NWs and the porphyrin, most likely of the form of Foster resonant energy transfer between inorganic donor and organic acceptor. CL spectroscopy results (Figure S2–S3, SI) confirm this idea (see discussion in SI). This same energy transfer is at the
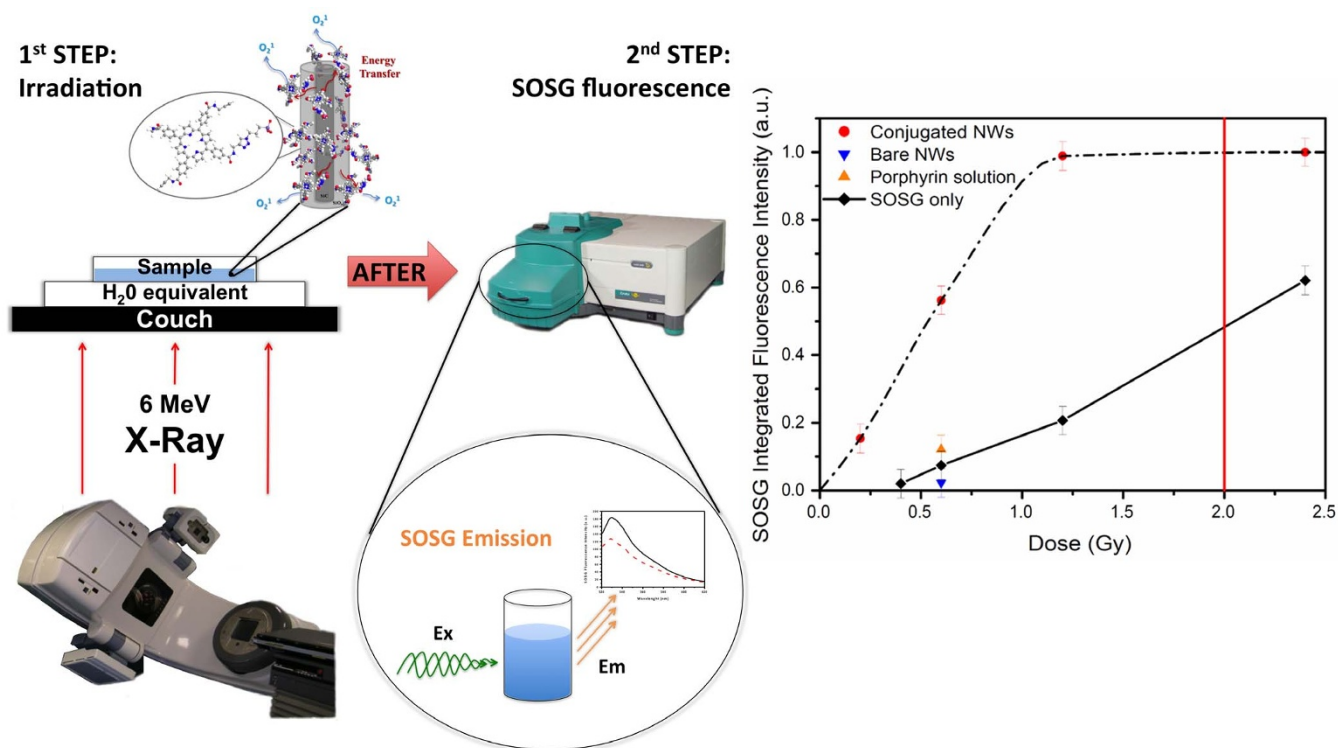
Figure 3 | $^1O_2$ production excited by X-Rays in a radiation therapy setup. Sketch of the experimental steps: a dish containing the sample solution is put on the couch and irradiated from the bottom (the picture of the linear accelerator has been taken at the Treatment Room of the Department of Medical Physics of Parma Hospital by one of the authors, Dr. F. Rossi, IMEM-CNR), then it is transferred to a spectrophotometer to acquire the fluorescence spectrum of the SOSG marker (picture taken at the Physics Department of Parma University by one of the authors, Prof. L. Cristofolini, Phys. Dept., Parma University). The plot reports the measured integrated fluorescence intensity, proportional to $^1O_2$ generated, as a function of the radiation dose. The experimental points are obtained from SOSG kit in water, with H_2TPACPP-functionalised NWs (red circles) or without NWs (black diamonds). The orange up-triangle at 0.6 Gy is the experimental point obtained from SOSG kit in a water solution of mere porphyrin, while the blue down-triangle is obtained from SOSG kit in a water suspension of NWs as grown. The usual dose for clinical treatment (2 Gy) is indicated by the red vertical line.

basis of the proposed application exploiting the singlet oxygen generation to induce oxidative stress in cancer cells.

The efficiency of the hybrid NW-H_2TPACPP system as a source of singlet oxygen ($^1O_2$) was tested by exposing the nanowires in water solution to 6 MV X-Rays in a clinical Linac Varian setup for radiation therapy (Figure 3). The singlet oxygen generation was revealed by a marker kit (Singlet Oxygen Sensor Green, SOSG[20]), which shows a green fluorescence activated by interaction with $^1O_2$ and is highly selective to $^1O_2$ against other oxygen species (hydroxyl radicals, superoxide etc.). Representative fluorescence spectra of the SOSG marker as-received, irradiated in water without nanowires, and irradiated in water solution containing H_2TPACPP-functionalised NWs removed from the substrate (see experimental details) are reported as Figure S4 in SI. The enhancement of the green fluorescence in the SOSG after treatment with the conjugated nanowires exposed to radiation demonstrates its effective activation, related to the production of $^1O_2$ by the NW-H_2TPACPP system even in extremely low-dose irradiation conditions (0.4 Gy). On the contrary, no SOSG activation was observed in treatments with bare NWs, nor with mere porphyrin solution, confirming that the $^1O_2$ production requires the conjugated NW-porphyrin system and occurs through the self-lighted photodynamic process. To rule out a possible X-Ray induced amorphous-to-crystal transition of the SiO$_x$ layer, which is known to be cytotoxic in the crystalline phase, we performed TEM studies on NWs irradiated at different doses: 0.6, 1.2 and 2.4 Gy. We chose by purpose pure SiO$_x$ amorphous NWs, to avoid any crystalline spots related to SiC in the TEM diffraction pattern. On the basis of the experimental observation (see SI Figure S5, acquired on NWs irra-

diated at the highest dose), we exclude any crystallization of the amorphous layer.

The $^1O_2$ concentration, as deduced from the integrated intensity of SOSG fluorescence, increases steeply as a function of the dose released up to 1 Gy. The dose-response relationship is shown in Fig. 3, from extremely low dose values (fraction of Gy) to typical doses of radiation therapy in clinical cancer treatments ($\sim$2 Gy per each session). The response of the nanosystem suspension (NW-H_2TPACPP in water, red circles) is well above the control solution (SOSG kit alone in water, black diamonds) and almost 5 times higher than the mere porphyrin response at the same dose (free porphyrin diluted in water, orange up-triangle) as well as the NWs as grown (suspension in water, blue down-triangle).

The saturation in the SOSG fluorescence signal reached around 1Gy can be reasonably attributed to the finite capacity of SOSG molecules to detect $^1O_2$ immediately after it has been produced. This is limited on one side by the short lifetime of this species in water (4 μs[21]) and on the other side by the exchange- limited by diffusion- of SOSG molecules between the nanosytem surface and the bulk of the solution. Another possible explanation, which cannot be ruled out, but is deemed less probable, is that for some intrinsic reason the production of $^1O_2$ itself is limited. This could be the case only if the supply of O_2 molecules would be limited or if the conversion to singlet was irreversible, which seems to be unrealistic assumptions.

In vitro experiments were performed on A549 adenocarcinomic human alveolar basal epithelial cells (Figure 4), to test the efficiency of the NW-H_2TPACPP nanosystem for possible self-lighted photo-
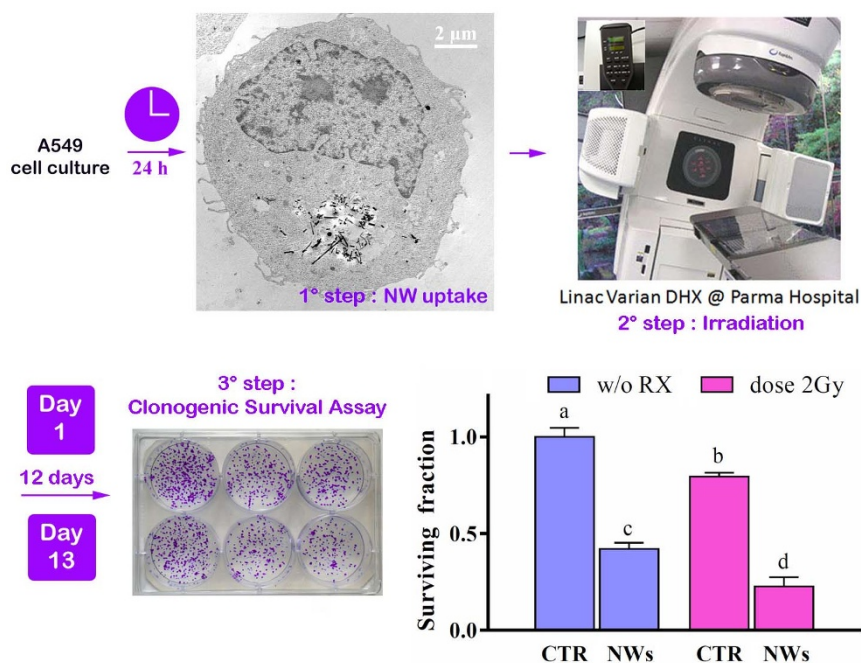
Figure 4 | Influence of H$_2$TPACPP-functionalised nanowires and radiation on A549 cells. Sketch of the experimental steps: the incubated cells uptake and internalize the NWs during the first 24 h, and are then irradiated in the radiation therapy setup (the picture has been taken by one of the authors, Dr. G. Benecchi, at the Treatment Room, Parma Hospital). Clonogenic survival assay is performed and colonies are stained after 12 days. The histograms, normalised to the control cells, report the surviving fraction of cells treated only with the NW-H$_2$TPACPP (50 μg/ml), only with radiation (2 Gy) or in combination of NW-H$_2$TPACPP and radiation. Columns: mean of three determinations; Bars: Standard Deviation. Each letter indicates a different level of significance ($p < 0.05$) after ANOVA followed by post-hoc test.

dynamic therapy. Our previous studies[11] demonstrated that A549 cells incubated with the NWs are able to actively internalize them, mainly for macropinocytosis, and that after 24 h an almost complete NW uptake and compartmentalization is observed (Figure 4, top-center). For the present study, A549 cells were incubated with H$_2$TPACPP-conjugated NWs and irradiated after 24 h with 6 MV X-Rays at the dose of 2 Gy (Figure 4, top-right), chosen accordingly to the standard conditions of clinical radiation therapy (single session). After treatment, a clonogenic survival assay (Figure 4, bottom) was performed: cells were cultured for 12 days and then examined to verify whether the NW-H$_2$TPACPP nanosystem was able to enhance the effects of the ionizing radiation and to inhibit the cell proliferation. The histograms indicated that H$_2$TPACPP-conjugated nanowires affect the survival of A549 cells, either under or without irradiation. The most striking result is that the cell plating efficiency after the radiation treatment is significantly lower for cultures incubated with the NWs than for control cells. To stress the effectiveness of our approach, an additional experiment has been performed at increased NW concentration (100 and 500 μg/ml) and at increased dose (6 Gy, single shot), evidencing a remarkable reduction of the adenosine triphosphate (ATP) intracellular amount, which is directly correlated to the cellular viability (see SI Figure S6). As for bare core/shell NWs, it has been shown in a previous paper from some of the coauthors[11] that they are cytocompatible and their internalization (without X-Ray irradiation) do not induce any significant reduction of the colony forming ability, as evaluated by clonogenic survival assay after 10 days.

This study demonstrates that the NW-H$_2$TPACPP nanosystem has an additive antiproliferative effect compared to irradiation alone at the selected dose. Furthermore, these results have been obtained with an irradiation time of 20 sec, which is significantly shorter than the standard clinical treatment times (40 sec with single, 90 sec with multiple irradiation fields). This shortening of the irradiation time is extremely relevant for minimizing target missing due to patient movements and reducing the psychological and physical discomfort due to the immobilization inside the isolated treatment room.

Methods

Synthesis of H$_2$TPACPP. According to a literature procedure[22], EDCI (146 mg, 0.76 mmol) and HOBt (103 mg, 0.76 mmol) were added to a solution of H$_2$TCPP (100 mg, 0.126 mmol) in 4 ml of anhydrous DMF. After stirring for 30 min, propargylamine (36 μl, 0.56 mmol) and DMAP (68 mg, 0.56 mg) dissolved in 1 ml of anhydrous DMF were added. The reaction mixture was stirred at room temperature for 24 h. Then the solvent was evaporated under vacuum giving a purple semisolid. AcOEt (50 ml) and water (50 ml) were added, and the organic phase was washed with water (50 ml × 3) and dried over anhydrous Na$_2$SO$_4$. The solvent was evaporated and the column chromatography of the solid, using CH$_2$Cl$_2$/MeOH (90 : 10) as eluant, afforded the product as a purple solid (71 mg, 60%). ^{1}H NMR (300 MHz, DMSO-d_6) δ 9.39 (4H, t, $J = 5.4$ Hz, NH), 8.86 (8H, s, βH), 8.34 (16H, m, ArH), 4.24 (8H, m, CH$_2$), 3.23 (4H, t, J = 2.3 Hz CCH), −2.92 (2H, s, NH). ^{13}C NMR δ 166.4, 144.6, 134.7, 133.9, 126.4, 119.9, 81.9, 73.5, 29. MALDI-TOF MS *m/z* calculated: 939.043, *m/z* found: 939.329.

Functionalization of nanowires with of 3-azidopropyltrimethoxysilane. The silica shell surface of the NWs was first activated boiling the wafer covered by NWs in 20 ml HCl conc. for 2 h. After washing with water to neutral pH, the sample was washed with acetone and dried in the air. Then, it was placed in a 50 ml round bottom flask and covered with toluene (about 10 ml). A solution of freshly prepared 3-azidopropyltrimethoxysilane[23] (2 μl of a solution 5 mM in toluene) was added and the reaction was heated at reflux under stirring overnight. After cooling, the nanowires were thoroughly washed with dry toluene, with acetone and dried in air.

NWs conjugation with porphyrin. The wafer covered by the nanowires bearing azide groups was placed in a 50 ml round bottom flask containing the H$_2$TPACPP porphyrine (16 mg), and was covered with DMSO (about 7–10 ml). The reaction was carried out at 130°C for 24 h to obtain the triazole ring formation. The samples were washed with DMSO, acetone and dried in the air. Last, the nanowires were removed (detached) from the support using a ultrasound microtip in acetone (Misonix Sonicator S4000, 5 W) and were recovered from the solvent by ultracentrifugation (14000 Hz).

Material characterization. Electron microscopy analyses of the as-grown NWs were performed in a Field-Emission SUPRA40 Zeiss SEM equipped with a GEMINI FESEM detection column, and in a Field–Emission JEOL JEM-2200FS TEM

microscope operated at 200 kV. For TEM observations, nanowires were transferred from the substrate by gentle rubbing on holey carbon-coated copper grids.

UV-VIS absorption spectra in the spectral range 350–700 nm have been recorded by a Jasco V550 double-source, double-beam spectrophotometer equipped with a photomultiplier detector (Hamamatsu, R928) and a VT unit. Temperature was kept constant to 25°C.

Fluorescence spectra were acquired with an ad-hoc built microfluorescence setup built around a TRIAX320 Horiba/Jobin-Ivon single pass monochromator. Excitation light was provided by a DPSS laser (CNI-Laser MBL-III-473-100-3 emission wavelength 473 nm, 100 mW maximum power, 1.2 mm spot size, beam divergence < 1.5 mrad) filtered with a 10 nm bandpass filter (Semrock FF01-473/10-25) and entering a microscope head equipped with an Olympus ULWD50 long focal 50× objective (N.A. 0.55). Fluorescent light, collected in backscattering geometry, was filtered with a 473 nm edge filter (Semrock BLP01-473R-24), analyzed by the TRIAX monochromator and detected by a peltier cooled CCD detector operated with our software built in the Matlab® computing environment. Typical integration times ranged from 1 to 30 seconds with maximum power density on the sample 1–2 mW/μm^2. No photobleaching effect was observed in these conditions.

Radiation therapy. The Varian Clinac 6 MV linear accelerator of Parma Hospital was used for radiation therapy treatments. Petri dishes, multi-well plates or cell culture dishes to be irradiated were placed on the couch over a 30 × 30 × 1.5 cm plastic water slab. The gantry of the accelerator was rotated by 180° and the irradiation field was set to 10 × 10 cm², with a source-skin distance (SSD) of 1 m. The dose rate was kept constant to 600 monitor units per minute, i.e. 6 Gy/min, for all the experiments.

Singlet oxygen detection. For the detection of the $^1O_2$ species, the Singlet Oxygen Sensor Green (SOSG, Life Technologies), a reagent based on fluorescein bound to a dimethylanthracene derivative, was employed. A stock solution (5 mM, in methanol) was prepared immediately upon receipt; a working solution (5 μM, in water) was prepared for each experiment.

To test the $^1O_2$ production, a set of NWs (2 mg) was dispersed in a given aliquot (500 μL) of the SOSG working solution and the solution was then exposed to radiation at 6 MV (radiation therapy protocol described above). After irradiation, the NWs were separated through ultra-centrifugation and 200 μL of the remaining solution were sampled for fluorescence analysis. For each run, the fluorescence spectra were acquired on the as-prepared solution, the irradiated solution, and the irradiated solution treated with NWs. The spectrum of the not irradiated aliquot was acquired as a reference signal of the SOSG marker, while the spectrum of the irradiated aliquot as a background for the signal of the irradiated aliquot with NWs.

The fluorescence spectra were acquired by a high sensitivity Varian Cary Eclipse spectrophotometer, equipped with a Xenon flash lamp. The signal was collected with a photomultiplier tube in the range 520–620 nm, in backscattering geometry, from 200 μL of the sample solution placed in a 96-well plate. The excitation wavelength was set at 505 nm, accordingly to SOSG data sheets, and the sample was illuminated only during the acquisition time (about 1 min).

Cell culture and viability assays. RPMI 1640 medium and reagents for cell culture were purchased from Gibco, disposable sterile plastics were purchased from Costar, all other reagents were from Sigma Aldrich.

The human NSCLC cell line A549 was maintained in RPMI 1640 medium supplemented with 10% fetal bovine serum, under a humidified atmosphere of 5% CO_2 at 37°C. The effects of H_2TPACPP-functionalised nanowires alone or in combination with X-rays were tested by means of clonogenic survival assay. Briefly, exponentially growing A549 were incubated for 24 h with NWs and then exposed to radiation therapy at 2 Gy. Appropriate numbers of cells were seeded in triplicate in 6-well plates and cultured for 12 days. After this period, the colonies were fixed with methanol:acetic acid (3 : 1, v/v), stained with crystal violet and scored as survivors when constituted by more than 50 cells. Unirradiated cultures were processed in the same experiment. The surviving fractions were calculated relative to the mean plating efficiency of cells untreated with NWs and unirradiated.

Intracellular levels of ATP were quantified by CellTiter-Glo® Luminescent Cell Viability Assay (Promega Corporation, Madison, WI, USA), according to the manufacturer's recommendations. Luminescence intensity was detected by a Cary Eclipse fluorescence spectrophotometer (Varian, Inc., Palo Alto, CA, USA) and normalized against control values.

1. Linkov, I., Bates, M. E., Canis, L. J., Seager, T. P. & Keisler, J. M. A decision-directed approach for prioritizing research into the impact of nanomaterials on the environment and human health. *Nature Nanotech.* **6**, 784–787 (2011).
2. Ferrari, M. Cancer Nanotechnology: opportunities and challenges. *Nature reviews/Cancer* **5**, 161–171 (2005).
3. Xia, Y. Nanomaterials at work in biomedical research. *Nature Mater.* **7**, 758–760 (2008).
4. Zrazhevskiywa, P., Senawb, M. & Gao, X. Designing multifunctional quantum dots for bioimaging, detection, and drug delivery. *Chem. Soc. Rev.* **39**, 4326–4354 (2010).
5. Doane, T. L. & Burda, C. The unique role of nanoparticles in nanomedicine: imaging, drug delivery and therapy. *Chem. Soc. Rev.* **41**, 2885–2911 (2012).
6. Chen, W. & Zhang, J. Using Nanoparticles to Enable Simultaneous Radiation and Photodynamic Therapies for Cancer Treatment. *J. Nanosci. Nanotech.* **6**, 1159–1166 (2006).
7. Juzenas, P. *et al.* Quantum dots and nanoparticles for photodynamic and radiation therapies of cancer. *Adv. Drug Deliv. Rev.* **60**, 1600–1614 (2008).
8. Liu, Y., Chen, W., Wang, S. & Joly, A. L. Investigation of water-soluble x-ray luminescence nanoparticles for photodynamic activation. *Appl. Phys. Lett.* **92**, 043901 (2008).
9. DeRosa, M. C. & Crutchley, R. J. Photosensitized singlet oxygen and its applications. *Coord. Chem. Rev.* **233–234**, 351–371 (2002).
10. Bonnett, R. Photosensitizers of the Porphyrin and Phthalocyanine Series for Photodynamic Therapy. *Chem. Soc. Rev.* **24**, 19–33 (1995).
11. Cacchioli, A. *et al.* Cytocompatibility and cellular internalization mechanisms of SiC/SiO₂ Nanowires. *Nano Letters* **14**, 4368–4375 (2014).
12. Fabbri, F. *et al.* Enhancement of the core near-band-edge emission induced by an amorphous shell in coaxial one-dimensional nanostructure: the case of SiC/SiO₂ core/shell self-organized nanowires. *Nanotechnology* **21**, 345702 (2010).
13. Rossi, F. *et al.* Structural and Luminescence Properties of HfO₂ Nanocrystals grown by Atomic Layer Deposition on SiC/SiO₂ Core/Shell Nanowires. *Scripta Materialia* **69**, 744–747 (2013).
14. Fabbri, F. *et al.* Optical properties of hybrid T₃Pyr/SiO₂/3C-SiC nanowires. *Nanoscale Research Letters* **7**, 680 (2012).
15. Bigi, F., Moroni, L., Maggi, R. & Sartori, G. Heterogeneous enantioselective epoxidation of olefins catalysed by unsymmetrical (salen)Mn(III) complexes supported on amorphous or MCM-41 silica through a new triazine-based linker. *Chem. Commun.* **7**, 716–717 (2002).
16. Bigi, F., Corradini, A., Quarantelli, C. & Sartori, G. Silica-bound decatungstates as heterogeneous catalysts for H₂O₂ activation in selective sulfide oxidation. *J. Catal.* **250**, 222–230 (2007).
17. Gouterman, M. Spectra of Porphyrins. *J. Molecular Spectroscopy* **6**, 138–163 (1961).
18. Gouterman, M. & Wagniere, G. H. Spectra of Porphyrins. Part II, Four Orbital Model. *J Molecular Spectroscopy* **11**, 108–127 (1963).
19. Liu, Y., Zhang, Y., Wang, S., Pope, C. & Chen, W. Optical behaviors of ZnO-porphyrin conjugates and their potential applications for cancer treatment. *Appl. Phys. Lett.* **92**, 143901 (2008).
20. SOSG kit, produced by Molecular Probes and commercialized by Life Technologies, product information: http://tools.lifetechnologies.com/content/sfs/manuals/mp36002.pdf ("Singlet Oxygen Sensor Green Reagent", revised 30/01/2004. Date of access: 12/05/2013).
21. Egorov, S. Y. *et al.* Rise and decay kinetics of photosensitized singlet oxygen luminescence in water. Measurements with nanosecond time-correlated single photon counting technique. *Chem. Phys. Lett.* **163**, 421–424 (1989).
22. Gianferrara, T. *et al.* Ruthenium-Porphyrin Conjugates with Cytotoxic and Phototoxic Antitumor Activity. *J. Med. Chem.* **53**, 4678–4690 (2010).
23. Meng, D. *et al.* Grafting P₃HT brushes on GO sheets: distinctive properties of the GO/P₃HT composites due to different grafting approaches. *J. Mater. Chem.* **22**, 21583–21591 (2012).

Acknowledgments

Author contributions

G.S. and F.R. conceived the idea for the manuscript and coordinated the experiments. M.N., S.C.D. and G.A. grew the nanowires. E.B. and F.B. performed the porphyrin synthesis and chemical characterization and developed the nanowire-porphyrin conjugation process. T.R. and L.C. conducted the spectroscopic characterization and the measurements on SOSG solutions. F.F. conducted the CL experiments. S.P. and R.A., under the supervision of M.G. and A.M., conducted the *in-vitro* experiments on cell cultures. G.B. and C.G. coordinated the irradiation treatments in the radiation therapy hospital laboratory. S.I. contributed to the project management. All the authors contributed to writing and approved the paper.

Additional information